Journal of General Practice
ISSN: 2329-9126

Loiselle et al., J Gen Pract 2014, 2:4
DOI: 10.4172/2329-9126.1000168

Review Article Open Access

Assessing the Efficiency of the Diabetic Heart at Subcellular, Tissue and Organ Levels

Denis S Loiselle[1,3*], June-Chiew Han[3], Kimberley M Mellor[1,3], Toan Pham[1,4], Kenneth Tran[3], Soyeon (Eden) Goo[1,3], Andrew J Taberner[1,2] and Anthony JR Hickey[4]

[1]*Department of Physiology, The University of Auckland, Auckland, New Zealand*

[2]*Department of Engineering Science, The University of Auckland, Auckland, New Zealand*

[3]*Auckland Bioengineering Institute, The University of Auckland, Auckland, New Zealand*

[4]*School of Biological Sciences, The University of Auckland, Auckland, New Zealand*

[*]**Corresponding author:** Denis Loiselle, Department of Physiology, The University of Auckland, Auckland, New Zealand, Tel: 64-9-373-7599; E-mail: ds.loiselle@auckland.ac.nz

Received date: May 01, 2014, **Accepted date:** Jun 26, 2014, **Published date:** Jun 30, 2014

Abstract

In this review, we focus on the diabetic heart rather than the vascular complications of diabetes. Focus is further narrowed to a specific, but widely used, animal model: the diabetic rat heart in which diabetes has been induced by a single injection of streptozotocin. Our experimental approach is primarily biophysical and ranges from measurements made in isolated working whole-hearts, to those made from isolated left-ventricular tissues and mitochondria. Our interest is on the effect of severe diabetes on cardiac energetics, in terms of efficiency of cardiac work performance, ATP synthesis and oxygen consumption. By designing experiments to test the energetic performance of the heart and its trabeculae across a wide range of protocols, we have revealed the dependence of efficiency on afterload. This has allowed us to clarify a long-standing uncertainty in the literature; whereas the diabetic heart is unable to work against high afterloads, it nevertheless retains normal peak efficiency. But a further anomaly has been revealed. Whereas there is no evidence that the diabetic myocardium loses peak mechanical efficiency, its mitochondria demonstrate a decreased P:O ratio - i.e., a decreased bioenergetic efficiency. This decrease is consistent with an increase in the rate of production of reactive oxygen species, together with elevated proton leakage across the inner mitochondrial membrane at near maximal phosphorylating respiration states.

Keywords: Cardiac oxygen consumption; Pressure-volume work; Myocardial heat production, Force-length work, Mitochondrial efficiency

Preamble

Readers of the Journal of General Practice will scarcely need to be reminded that diabetes is a leading cause of death in both the 'developed' and 'developing' world [1]. New Zealand is no exception. We do have something of a unique situation, however, since the burden falls disproportionately on the Maori & Polynesian populations, with both the prevalence and the death rates approaching double those of Pakeha (http://www.maoridiabetes.co.nz/). Given the strong link between obesity and diabetes, the high rates of obesity in New Zealand (31% of adults in 2013) is of increasing concern (http://www.health.govt.nz/our-work/diseases-and-conditions/obesity/obesity-key-facts-and-statistics).

There have been a number of excellent reviews on the subject of diabetes [2-5], surely the most unique of which is that authored by Gottlieb [6], dealing with clinical and epidemiological issues. Since we are neither clinicians nor epidemiologists but rather, physiologists, biophysicists and bioengineers, we offer a different point-of-view. Our motivation commences from the knowledge that upwards of 80% of overall morbidity and mortality associated with diabetes is attributable to cardiovascular disease, involving both the arterial/arteriolar system and the myocardium per se. Specifically, we focus on the 'diabetic heart' first described by Rubler et al. [7] from four diabetic patients who had died of diabetic glomerulosclerosis and whose hearts were hypertrophied but showed no signs of arterial disease at autopsy. It is now generally accepted that a specific diabetic cardiomyopathy exists, independent of vascular complications [8]. In our case, the phrase 'diabetic heart' implies the heart of an animal rendered diabetic by some means.

Animal Models of Diabetes

Whereas ultimate interest must remain on the diabetic human heart, it is experimentally fortuitous that animal models exist. In fact, there are a plethora of animal models (for a comprehensive review, see Gomes et al., 2013). Some have been induced by genetic manipulation (db/db mouse, ob/ob mouse, OVE26 mouse, GLUT4-KO mouse), while others have arisen from spontaneous genetic mutation (Zucker Diabetic Fatty (ZDF) rat, Zucker Fatty (ZF) rat, Goto-Kakizaki rat), dietary intervention (high fructose diet, high fat diet, high sucrose diet), or pharmacological intervention (streptozotocin, alloxan). Our particular choice has been the heart of the streptozoticin (STZ)-treated rat. It is an excellent model of Type I diabetes (since the pancreatic Islets of Langerhans have been destroyed), but it has the added advantage of also mimicking a number of features of Type II diabetes in human patients [9].

A feature of STZ-induced diabetes that renders it particularly attractive to experimentalists is its simplicity. Some six to eight weeks following a single injection, rats have full-blown diabetic symptoms including blood glucose concentrations in excess of 25 mM. The

cardiac complications evident in the STZ rat mimic those observed clinically: hypertrophy, fibrosis and (of particular relevance to this review) prolonged relaxation. The model thus provides an important experimental opportunity for new investigations of the mechanisms of cardiac pathology in diabetes.

One such mechanism, which has not been without controversy, is the proposal that cardiac dysfunction in diabetes is explained by a reduction in efficiency of the heart pump. We consider that our recent investigations have advanced understanding of this issue. Indeed, our findings form the focus of this Review. A secondary objective is to demonstrate the applicability of animal models in this endeavour. But, first, a brief overview of the characteristics of the diabetic heart.

Characteristics of the Diabetic Heart

Diabetic cardiomyopathy is a distinct cardiomyopathy [7-11]. Indeed, in a substantial proportion of otherwise healthy type 2 diabetics, subclinical left ventricular dysfunction presents prior to development of overt signs of coronary vascular disease [10,12]. Abnormal filling of the left ventricle, consistent with a decrease of left-ventricular compliance [13-15] is an early sign of cardiac pathology in the diabetic heart [16,17]. The prevalence of diastolic dysfunction in type 1 and type 2 diabetes may be as high as 40-75% without overt coronary artery disease [18]. Diastolic dysfunction has been reported in type 1 diabetic adolescents [19-22]. These patients have neither vascular nor haemodynamic complications. Nevertheless, they exhibit a primary myocardial defect. Progression from diastolic to systolic dysfunction in late-stage diabetes is observed clinically, and overlap of both forms of failure is common [23]. In type 2 diabetic patients, myocardial systolic dysfunction is independently associated with glycated hemoglobin level [10].

The Meaning of Cardiac Efficiency

'Efficiency', in any field, implies the notion of 'output' for a given amount of 'input'. The heart, like any other muscle, is a thermodynamic machine; it is capable of directly converting biochemical energy into mechanical energy. A reduction of its efficiency implies either/both diminished ability to perform work, for a given amount of metabolic input, or increased metabolic energy expenditure for a given work output. In either case, decreased efficiency of the heart signifies that something is amiss with its internal machinery. Malfunction can appear on either the 'input' limb (i.e., the production of ATP) or the 'output' limb (i.e., the consumption of ATP). It is possible to quantify the efficiency of both limbs of this 'production-consumption' cycle.

Mitochondrial efficiency

Mitochondria are plentiful in the heart, occupying some 30%-40% of myocyte volume [24]. Input to a mitochondrion is in the form of O_2 and substrates derived from glucose, lipids and amino acids to form acetyl-CoA, ADP and inorganic phosphate (Pi). The fundamental output is ATP, which is either utilised directly or acts to rephosphorylate creatine to creatine phosphate, which functions both as a 'high energy store' and an 'energy shuttle' [25,26]. The citric acid cycle and the electron transport chain establish a chemi-osmotic gradient of protons across the inner mitochondrial membrane [27]. Harnessing of the free energy of the proton gradient (Figure 1) dictates the efficiency of ATP generation from ADP and Pi by the membrane-bound ATP-ADP synthetase [28-31].

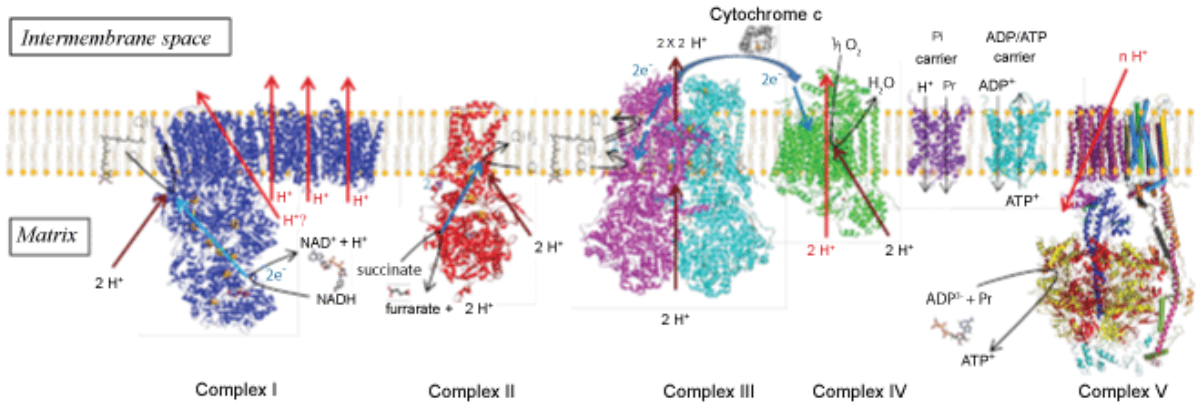

Figure 1: Mitochondria electron transport and oxidative phosphorylation systems NADH and $FADH_2$ are oxidised at Complexes I and II, with electrons donated to reduce ubiqinone (Q) to ubiquinol (QH_2) and transferred to Complex III. The upwardly facing red arrows indicate the direction of proton transfer from the matrix across the inner membrane into the inter-membrane space between the inner and outer mitochondrial membranes. Transfer of two electrons from Complex III to Complex IV, via Cytochrome C Oxidase, then reduces ½O_2 to H_2O. Note that Complex II does not contribute directly to the proton gradient but does so indirectly at Complexes III and IV. Complex V (the ADP-ATP synthetase) then exploits the electrochemical proton gradient to synthesise ATP from ADP and Pi. ATP is then exchanged for ADP across the inner mitochondrial membrane via the Adenine Nucleotide Transporter (ANT, ATP/ADP carrier. Pi (inorganic phosphate) is also maintained via the proton gradient. [Reproduced from Mazat et al. (2013) Critical Review: Mitochondrial Energetic Metabolism–Some general principles, IUBMB Life 65(3): 171-179 (2013), with permission of the authors and the Editor of the International Union of Biochemistry and Molecular Biology Life].

Since the output of this system is ATP and the input is oxygen, it is natural to define the efficiency of the 'metabolic chain' as the ratio of the number of moles of ATP produced per mole of oxygen consumed. Biochemists typically measure the O_2 flux and infer the ATP by monitoring transitions in respiration rates (or states 2 to 3 to 4) following the addition and depletion of limiting amounts of ADP. A simple P:O ratio is derived, where P signifies 'ATP' and O signifies molecular oxygen. Biophysicists, on the other hand, typically measure only the consumption of oxygen (VO_2), converting it to units of energy using a conversion factor known as the 'energetic equivalent of oxygen'.

The energetic equivalent of oxygen: This quantity, classically evaluated as 20 kJ per litre of oxygen (marginally less for fatty acids), arises from an experiment that is conceptually and technically very simple–namely, the complete oxidation of glucose in a bomb-calorimeter. Readers may recall that this yields 36-38 molecules of ATP, giving the classical P:O ratio of 3.0-3.2. However, re-evaluation of these quantities over the past decade has led to their reduction in magnitude. The revised values are 29.4-29.9 ATP/glucose producing an updated P:O ratio of 2.4-2.5 [32,33]. This reduction of efficiency of approximately 18% is primarily attributable to more recent experiments being conducted at physiological temperature (37°C) rather than at 'standard' (20°C) or 'room' (24°C) temperatures. At body temperature, the inner mitochondrial membrane becomes more permeable to protons and this diminishes the apparent efficiency of oxidative phosphorylation (OXPHOS).

The measurement of mitochondrial efficiency

Recent technological advances have reinvigorated the measurement of mitochondrial energetics, largely through the application of fluorescence-based measures that permit analysis of reactive oxygen species (ROS), mitochondrial membrane potential and ATP synthesis [34-36]. 'Substrate-inhibitor-titration' protocols have been developed [37-41]. These protocols have provided approaches that permit dissection of the electron transport system (ETS) and OXPHOS. Essentially, different protocols measure O_2 uptake in a high-resolution respirometer while metabolic substrates, or specific poisons, are added in an order generally specified by the 'linear' electron-stripping arrangement of Complexes I to IV. One of our general experimental protocols, which is coupled to the measurement of ATP, is as follows.

Measurement of the rate of leak respiration: Complex I-mediated "leak" respiration can be determined using saturating levels of Pi and substrates that generate NADH (eg. malate, glutamate and pyruvate). Since ADP is absent, any resulting respiration is due to proton conductance across the inner membrane, or electron slippage in the ETS. If saturating ADP is added, OXPHOS is activated and a ratio of Leak/OXPHOS can provide a measure of the potential turnover of oxygen that does not contribute to ATP synthesis. This can also be performed following the addition of succinate (Figure 2). Following the addition of succinate, $FADH_2$ is formed (bound within Complex II) and is re-oxidised to donate electrons to the ETS. Following the addition of saturating ADP, OXPHOS is activated. The ratio of Leak/OXPHOS can be derived, and this provides a measure of the potential turnover of oxygen that does not contribute to ATP synthesis, i.e. efficiency. While useful, this ratio assumes that the proportion of leak remains constant, and does not decrease as phosphorylation commences, when the membrane potential declines. Leak ratios are also lower with Complex II substrates as the redox potential of $FADH_2$ is too low to mediate proton pumping (unlike Complex I, see Figure 1), and therefore Complex II is less "coupled" to OXPHOS. The combination of Complex I and II substrates results in an intermediary Leak/OXPHOS ratio, or coupling in terms of the P:O ratio, but this likely reflects mitochondrial function and efficiencies *in vivo*, as both sets of substrates are present in vivo [42]. Electron transfer flavoproteins (ETF) involved in fatty acid β-oxidation, are also FAD containing enzymes and, like Complex II, are also less coupled. Therefore the Leak respiration rate and efficiency vary with substrate, and substrate contributions likely differ given that the diabetic heart has a greater dependence on lipid oxidation [43-45].

Leak and uncoupled respiration: Leak respiration results from different known and hypothetical sources. Those that are known result from proton conductance directly through the inner membrane, through Uncoupling Proteins (UCPs) [46,47], and the adenine nucleotide transporter (ANT, Figure 1). In addition, some lipids can act as uncoupling agents. Less understood sources of leak may result from electron slippage, and some of this may be attributed to reactive oxygen species (ROS) production from the ETS, yet this likely contributes a minimal loss of efficiency [34]. UCPs are positively regulated by the reactive oxygen species: $O_2^{\cdot -}$, and their activation will decrease coupling efficiency [46,47]. The source of leak respiration can be further explored by addition of oligomycin, a blocker of the F_1F_0-ATPase, and/or atracyloside or carboxy atractyloside. While both inhibit OXPHOS, the atractyloside compounds also inhibit proton conductance through ANT. Guanine Diphosphate (GDP) is also a potent inhibitor of UCPs [48]. Therefore the OXPHOS components of leak can be dissected.

Testing limits on the OXPHOS system: Repeated titrations of uncoupling agents such as dinitrophenol, or more commonly carbonyl cyanide-p-trifluoromethoxyphenylhydrazone (FCCP), are used to uncouple and depolarise mitochondria [49]. This then provides a measure of the ETS capacity relative to the OXHPHOS, and ratios ETS/OXPHOS. Typically there is an excess capacity of the ETS/OXPHOS. A decrease in this ratio can indicate decreased ETS capacities [39]. Preliminary data from our group indicates that there is less ETS capacity in STZ-diabetic rat heart mitochondria and similar findings have been reported by others [50]. In this regard, it is germane to note that cardiac mitochondrial respiration is regulated by nitric oxide [51], thereby likely limiting ATP synthesis *in vivo*, and that nitric oxide production is elevated in chronic states of cardiac disease [52].

Background respiration and Complex IV (Cytochrome *c* oxidase): Following the addition of antimycin A, respiration is inhibited at Complex III and this provides a measure of non-mitochondrial respiration. The addition of ascorbate and N,N,N',N'-Tetramethyl-p-Phenylenediamine (TMPD) supplies electrons to Complex IV (Figure 2).

Real-time measurement of ATP synthesis: Many studies of the diabetic heart have shown metabolic derangements at the level of the mitochondria (see the Review by Bugger and Abel [53]). One study, testing permeabilised fibres of type 2 diabetic human atrial appendage, showed altered (Complex I-supporting) lipid and glutamate flux [54]. Other studies, using animal models of type II diabetes mellitus, showed decreased OXPHOS capacities and P:O ratios [48,55,56], but see [57]. But the reported effects of diabetes on coupling efficiency have ranged from negligible to reduced [53]. Some of this variability may be attributable to the fact that, until recently, P:O ratios have been determined using sub-optimal amounts of ADP. This, in turn, limits

the maximal flux of respiration in the OXPHOS state, thereby restricting interpretation in the context of high work rates.

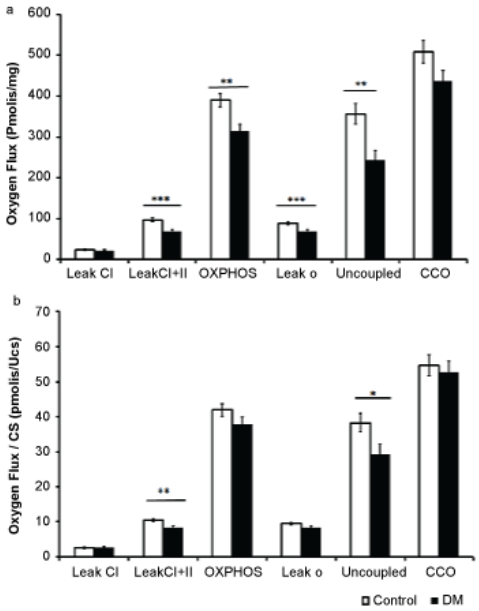

Figure 2: Mitochondrial respiration capacities in different respiration states of diabetic (black) and age matched control hearts (open). (a) Oxygen flux capacities per wet mass of cardiac homogenate were derived from ROS experiments. (b) Capacity relative to citrate synthase (CS) of 8-week diabetic rat hearts (black) and their age-matched controls (open). *Leak CI* (non-phosphorylating flux) was initiated with Complex I (CI) substrates glutamate, malate and pyruvate and Leak CI+II represents the leak respiration attributable to both CI and the Complex II (CII) substrate succinate. After addition of ADP, oxidative phosphorylation flux (OXPHOS) was measured. Leak CI+II was again measured after addition of oligomycin (Leak o). The mitochondria were uncoupled with FCCP ('Uncoupled'). Antimycin A was added to inhibit Complex III and oxidative flux was measured through cytochrome c oxidase (CCO) following TMPD and ascorbate addition. Paired student t-tests were used to test statistical significant difference between the Control and Diabetic groups ($^{*}P<0.05$, $^{**}P<0.01$, $^{***}P<0.005$, n=12 for both groups). [Unpublished results of Toan Pham.]

Methods have now been developed that permit fluorescence-based measurements of ATP/ADP exchange [58] under non-limiting conditions and we have integrated this system to examine ATP synthesis simultaneously with mitochondrial respiration. The magnitude of ATP/ADP exchange can be measured in real time by fluorometric quantitation of Mg^{2+} (Figure 3) which preferentially chelates ATP. We follow the fluorescence of the fluorophore Magnesium Green (MgG, "Molecular Probes"™) since Mg^{2+}-MgG fluorescence decreases as ATP is formed [58]. The inhibitors ouabain and blebbistatin are used to inhibit Na^{+}-K^{+} ATPase and the myosin heavy-chain [59], respectively. A sample (2 mg of tissue homogenate, or 0.125 mg/ml of mitochondrial protein) is added to Mg^{2+}-containing media within the oxygraph chambers and allowed to equilibrate. Substrates (pyruvate, glutamate, malate and succinate) are then added followed by excess Mg^{2+}-free ADP. The added ADP also serves as a reference/standard since, whereas ADP also binds Mg^{2+}, it does so with a 9-fold lower affinity and any ATP produced decreases the MgG fluorescence further. Separate experiments, titrating either ADP or ATP, are conducted to determine correction factors so that the ADP signal can be used as a calibration point. OXPHOS now proceeds and ATP production/turnover can be measured in real time with, and even without, oxygen [34]. An advantage of this approach is that ATP dynamics can be measured at saturating ADP concentrations, in pseudo-steady states and into anoxia. Oligomycin can then be added to determine the rate of mitochondrial ATP hydrolysis, as anoxic mitochondria become net ATP consumers. This provides insight into issues likely occurring in settings of cardiac infarct. Recent data indicate that, whereas type I diabetic rat heart have depressed OXPHOS capacity, anoxic mitochondrial ATP hydrolysis capacity matches that of normal heart mitochondria. That is, upon reperfusion, diabetic hearts will be at a greater ATP deficit than healthy hearts.

Measurement of rate of production of reactive oxygen species (ROS) simultaneously with respiration: An additional, although minor, loss of mitochondrial efficiency occurs through the loss of electrons from the ETS. The superoxide radical ($O_2^{\cdot -}$) is formed from molecular oxygen as a by-product of oxidation at mitochondrial Complex I and Complex III. In vivo, $O_2^{\cdot -}$ is normally degraded by superoxide dismutases (SOD) to hydrogen peroxide (H_2O_2), or consumed by antioxidants and antioxidant enzyme systems (which generally reduce H_2O_2 to H_2O and less harmful products) and by peroxidases and catalase to O_2 and H_2O [60].

Net ROS production can be measured simultaneously with respirational flux using the fluorophore Amplex Ultrared ("Molecular Probes"™). Addition of exogenous SOD can also enhance ROS detection. The combined mitochondrial H_2O_2 and exogenous SOD-derived H_2O_2 is then linked to horseradish peroxidase which, in turn, reacts with Amplex Ultrared to form a fluorescent product [35,61]. The production of H_2O_2 from various sources is shown in Figure 4a for samples of heart tissue from STZ-treated rats and their SHAM-injected controls. The relatively minor production of reactive oxygen species, is made apparent in Figure 4b, where the least activity is seen to occur during oxidative phosphorylation.

Does Diabetes Diminish Mitochondrial Efficiency?

This question has been addressed in a variety of ways for the past half century, with a remarkable degree of consensus.

Evidence from the literature

In an early paper, Parks et al. [62] showed a decrease in the P:O ratio of alloxan-induced type 1 diabetic rats, albeit from liver mitochondria. Comparable behaviour was reported for mitochondria isolated from the hearts of STZ-induced diabetic rats by Pierce and Dhalla [63]. Since those early studies, functional impairment of diabetic cardiac mitochondria has been reported in a variety of animal models: genetically diabetic mice [64], STZ-induced type 1 diabetic rats [65], insulin-resistant and obese mice [43,44] and Zucker Diabetic Fatty rats at submaximal rates of ADP-stimulated respiration [66], even prior to the development of symptoms of diabetic cardiomyopathy [67]. Our recent (unpublished) results (Figure 3) are in general accord.

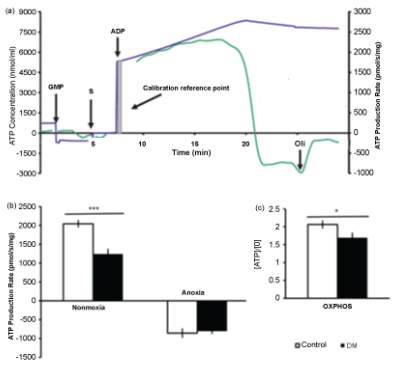

Figure 3: ATP production capacities per milligram of diabetic (black bars) and age-matched control hearts (open bars). (a) Respirational flux was followed in the presence of oxygen and CI and CII substrates ('GMP': glutamate, malate, pyruvate and succinate, 'S') followed by addition of Mg^{2+}-free ADP to initiate ATP synthesis (OXPHOS). Respiration was allowed to run into anoxia after which oligomycin (Oli) was added and background ATP hydrolysis signal subtracted. (b) Active or steady-state, P:O ratio was then determined from the rate of ATP synthesised relative to the flux of molecular oxygen in OXPHOS. (*P<0.05, **P<0.01, ***P<0.005, n=12 per group 8-week diabetic rat hearts and their age-matched Controls). [Toan Pham: unpublished results.]

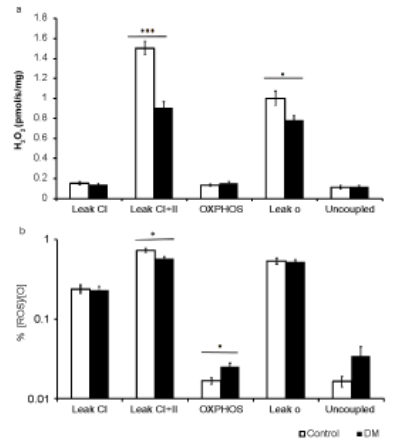

Figure 4: Reactive oxygen species (ROS) production of diabetic (black) and age matched control hearts (open). (a) Mean H_2O_2 (pmol H_2O_2 (s.mg)$^{-1}$) calibrated with a known amount of H_2O_2 in various mitochondrial states. (b) The [ROS]/[O] ratio was indexed as the amount of ROS production relative to respiration O flux in leak and OXPHOS states (*P<0.05, n=12 per group 8-week diabetic rat hearts and their age-matched Controls). [Toan Pham: unpublished results.]

Possible *modi operandi*

It has been recognised for half a century that diabetes is characterised by a reduction of glucose metabolism in favour of fatty acids [68]. That original study was done in the rat heart but the result has been shown to be equally valid in human patients suffering Type I diabetes [69]. It is this switch from carbohydrate to fatty acid metabolism that is presumed to diminish cardiac mitochondrial efficiency. Yet a number of causes have been touted and tested. Boudina and Abel [70] discuss various deleterious effects of increased fatty acid oxidation that characterise both Type I and Type II diabetes, among which is increased mitochondrial production of reactive oxygen species (ROS) including superoxide radicals known to be capable of activating uncoupling proteins [55]. The result of such a scenario would be a decrease of mitochondrial efficiency, since the proton gradient would be 'squandered' (Figure 1) and the ETS would demand more O_2. Boudina and Abel [71] further contend that the 'activating' action of reactive oxygen species "…amplify the hyperglycemia-induced activation of protein kinase C isoforms [and] increase formation of glucose-derived advanced glycation end-products". The hyperglycaemic setting of diabetes, combined with elevated levels of ROS, provides the ideal environment for glycation to occur–irreversible and obstructive attachment of an advanced glycation end product to a protein, adversely affecting protein structure and function.

Oxygen radicals, in particular, are expected to reduce mitochondrial efficiency by damaging proteins and lipid membranes, cardiolipin in particular [72], and elevating proton leak through uncoupling proteins [70]. But whatever the *modi operandi* of ROS in diminishing mitochondrial efficiency, it is sobering to learn that a high-fructose diet *per se* is capable of generating superoxide in the murine heart, despite only mild hyperglycemia and in the absence of overt cardiac dysfunction [73,74], thus supporting the contention that ROS-induced intracellular damage is an early manifestation of diabetic cardiac pathology. Over-consumption of fructose, particularly as a consequence of its insidious use as a sweetener in foods and soft-drinks, is implicated in the 'insulin resistance syndrome' and the 'obesity epidemic', which runs in parallel with the 'diabetes epidemic' [75].

The Output Efficiency of the Heart

Having dealt with the input (mitochondrial) efficiency of the heart, we now turn our attention to its output (work) efficiency. In order to do so, we first remind readers of the commonly-adopted partitioning of the total energy expenditure.

Partitioning of cardiac energy expenditure

The major division is between basal and suprabasal metabolic rate. The basal component requires that the heart be at rest. Since this does not occur during life, some experimental intervention (such as high K^+ arrest) is required for this measurement. The suprabasal moiety reflects the metabolic cost of the actively beating heart. This component of metabolism is again divided between the energy to activate contraction and the energy to effect contraction. The latter reflects the hydrolysis of ATP by crossbridge ATPase activity. The former includes the hydrolysis of ATP by the sarcolemmal Na^+-K^+ ATPase to restore transsarcolemmal ion gradients following the action potential, plus the cost associated with the uptake of Ca^{2+} by the sarcoplasmic reticular (SR) Ca^{2+}-ATPase. The SR is the internal store

of Ca^{2+} in the cell. This Ca^{2+} is released from the SR store and binds to contractile proteins, thereby inducing contraction. The SR Ca^{2+} ATPase transports the Ca^{2+} back into the SR thus allowing relaxation to occur.

Early studies [76,77] (for a review, see Cesario et al. [78]) attributed the diminished contractility of the diabetic heart to reduced Ca^{2+} release from the sarcoplasmic reticulum (SR). However, more recent studies of streptozotocin-induced diabetic hypertrophy [79,80] have shown no detectable diminution in magnitude of the 'Ca^{2+} transient'.

Because cardiac dysfunction in diabetes is not always linked to changes in the Ca^{2+} transient, we have focussed our attention downstream, on the mechanical behaviour, and energetic cost, of the Ca^{2+}-triggered, actin-activated, myosin ATPase of the contractile proteins. The acto-myosin complex is the principal consumer of metabolic energy in the cardiac myocyte. It directly converts the Free Energy of ATP hydrolysis into cycling of actin-myosin cross-bridges, thereby allowing shortening and force production by the sarcomeres. Our focus is on the efficiency of this energy transduction process [34]. We measure cardiac efficiency at two distinct levels: the isolated whole-heart and isolated ventricular trabeculae. In the former case, efficiency is given by the ratio of pressure-volume work to the energetic equivalent of oxygen [81]. In the latter case, efficiency is given by the ratio of force-length work to the sum of work and heat production [82-84]. We hope to demonstrate to readers the advantage of studying the diabetic myocardium at these two extreme levels of structural organisation of the heart. But, prior to embarking on that undertaking, we wish to dispel that notion that there are other, arbitrary, definitions of 'efficiency'.

"PVA 'efficiency": Many readers will have encountered the notion of PVA (pressure-volume-area) efficiency as introduced and extensively promulgated by Suga and colleagues [85-89]. The notion is based on the assumption that the area between the abscissa and the (linear) end-systolic pressure-volume relation quantifies the external work performed by the heart. The ratio of this 'work' term to the volume of oxygen consumed in performing it comprises 'PVA efficiency'. The notion is appealing but, in our view, fundamentally flawed for the following reasons. Firstly, efficiency should not be invariant with afterload. In particular it should be zero when no external work is performed–i.e., under both zero-load contractions and isovolumic contractions. But 'PVA efficiency' of the healthy heart is reported to be some 40%, independent of loading conditions [89]. Secondly, the numerator should not contain a component that correlates with twitch heat production, as recent experimental and theoretical analyses have shown to be the case [90,91]. Thus, whereas the ratio of PVA to VO_2 may be of clinical or other interest, we advocate that it no longer be referenced as a measure of cardiac efficiency.

In order to study the efficiency of the heart, we use isolated hearts and isolated trabecula preparations. These experimental models allow cardiac investigations without the complication of either neural or humoral input. Details of these two experimental approaches follow.

The isolated rat whole-heart model

In our experiments, an STZ-induced diabetic rat heart is excised under deep anaesthesia and mounted in a working-heart rig [34,81,84] in which preload and afterload can be varied independently. In order to avoid the vexing problem of variation of heart rate between specimens, the hearts are electrically paced at a rate in excess of their spontaneous beat frequencies. Aortic and coronary flows of a glucose-supplemented saline perfusate, together with their oxygen partial pressures, are measured continuously, allowing calculation of oxygen consumption (VO_2) at any desired combination of preload and afterload (Figure 5).

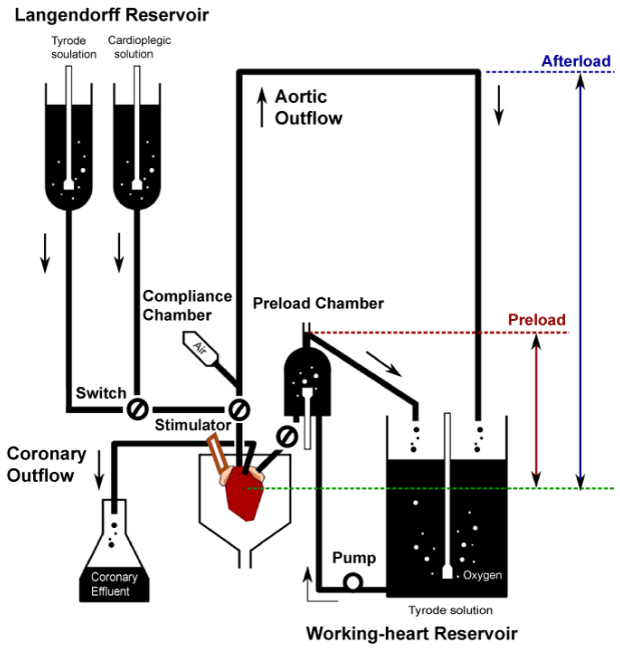

Figure 5: Schematic representation of the isolated heart perfusion apparatus, Indicated are the sources of oxygenated perfusate and the arrangements for independently varying preload and afterload. Note the parallel configuration for Langendorff-perfusion in order to measure basal oxygen consumption. In working-heart mode, the heart is stimulated electrically to contract at a frequency in excess of its spontaneous rate, while LV and aortic pressures, coronary and aortic flows and oxygen partial pressures are recorded continuously. [Reproduced, with modification, from PhD Thesis of Soyeon (Eden) Goo [92].]

Examples of (continuous) output from selected transducers located in the whole-heart apparatus are presented in Figure 6.

Whereas isovolumic contractions cannot be achieved (since the 'systemic' (aortic) and coronary (pulmonary arterial) flows are in parallel), they can be approximated by increasing the afterload to the point where the left ventricle is no longer capable of ejecting a stroke volume. Thus the metabolic energy demand can be examined over a very wide range of afterloads. This fact is crucial to many of our interpretations, as will be elaborated below.

The measured variables shown in Figure 6 form the basis of derived quantities of interest. For example, stroke volume is given by the quotient of total flow (aortic+coronary) and pacing frequency. External work is then calculated as the product of stroke volume and mean aortic pressure. Oxygen consumption (VO_2) is given by the product of coronary flow, the solubility of oxygen and the arterio-venous difference in partial pressure across the coronary circulation. Cardiac efficiency is then given by the ratio of pressure-volume work to VO_2. Calculated (and curve-fitted) values of work, oxygen

consumption and their ratio, cardiac efficiency, are shown in Figure 7 for Control and STZ-treated hearts.

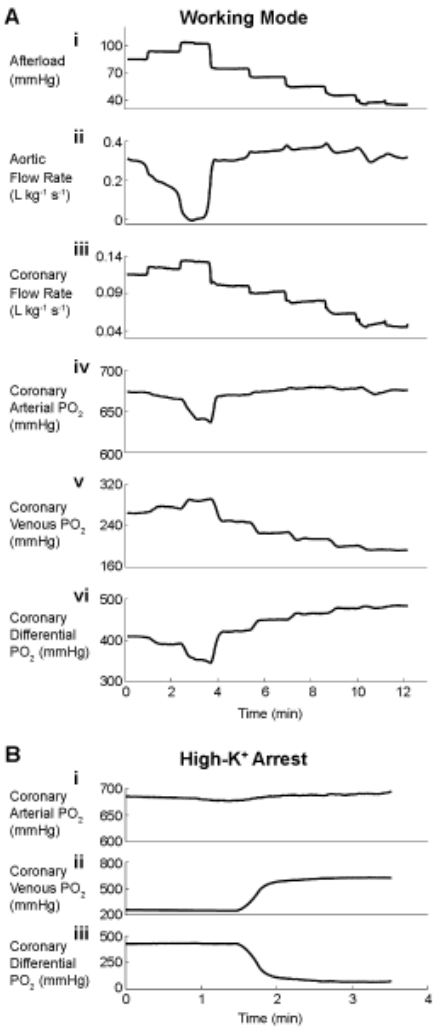

Figure 6: Original records from an isolated rat heart. A: working-heart mode; Panel i shows the aortic pressure recorded at 9 consecutive afterloads between 40 mmHg and 100 mmHg. Panels ii and iii show, respectively, the instantaneous aortic and coronary venous flow rates, normalised to the wet weight of the heart; Panels iv and v show coronary arterial and venous PO_2, respectively, while Panel vi shows the 'a-v difference'. The progressively increasing afterload-dependence of the trace in Panel vi reflects progressive coronary vasodilation. Instantaneous values in Panel vi, multiplied by the product of the rate of coronary flow and the solubility of oxygen, yields the myocardial oxygen consumption of the working heart. B: Langendorff-perfusion mode during experimentally-induced (26 mM K^+) cardiac arrest. Note the continued stability of arterial oxygen partial pressure (i) and the very much higher values in the coronary venous output (ii) vis-à-vis those observed in working-heart mode, reflecting the much lower rate of (basal) oxygen consumption (iii). [J-C Han: unpublished results.]

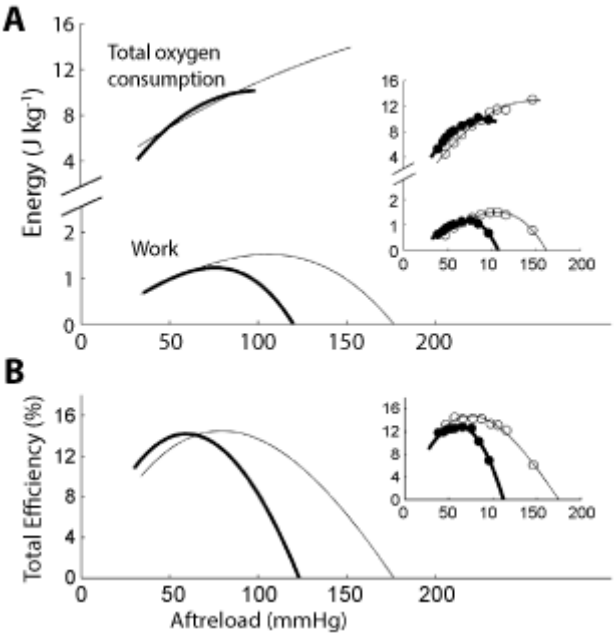

Figure 7: Mechano-energetic data from rat whole-heart experiments. A: Average total energy expenditure (VO_2 and work; note two different scales on the ordinate) and B: average total efficiency, of 17 Control (thin lines and open circles) and 16 STZ-diabetic (thick lines and filled circles) hearts. The insets show representative data from individual hearts. [Modified from Han et al. [84].]

As is evident in Figure 7, the ability of the heart to perform external, macroscopic, pressure-volume work (given by the product of stroke volume and mean aortic pressure, Panel A) is a complex function of after-load, being zero at both the origin and at the extrapolated isovolumic point, and peaking at some intermediate afterload. By contrast, the metabolic energy expenditure (indexed by VO_2, Panel A) has a roughly monotonic dependence on afterload. In consequence, the ratio of mechanical energy output to metabolic energy input (efficiency, ε_{Total}, Panel B) mimics the afterload-dependence of work. The subscript 'Total' on 'ε' signifies that we are including the total oxygen consumption of the heart and not merely its supra-basal value. If required, the basal rate of cardiac metabolism can be estimated by arresting the heart, commonly achieved by using either a high K^+ [93, 94] or a low Ca^{2+} [93,95] perfusate. Subtracting the basal oxygen consumption from the total clearly identifies the metabolic cost of activating contraction plus that of the work performance *per se*. Separation of the 'activation' component of work from the contractile component is not readily achieved in the whole heart, although Suga and colleagues developed a pharmacologically-based protocol [96,97] for its estimation. We take a different (non-pharmacological) approach as will be shown in the section on energetics of trabeculae.

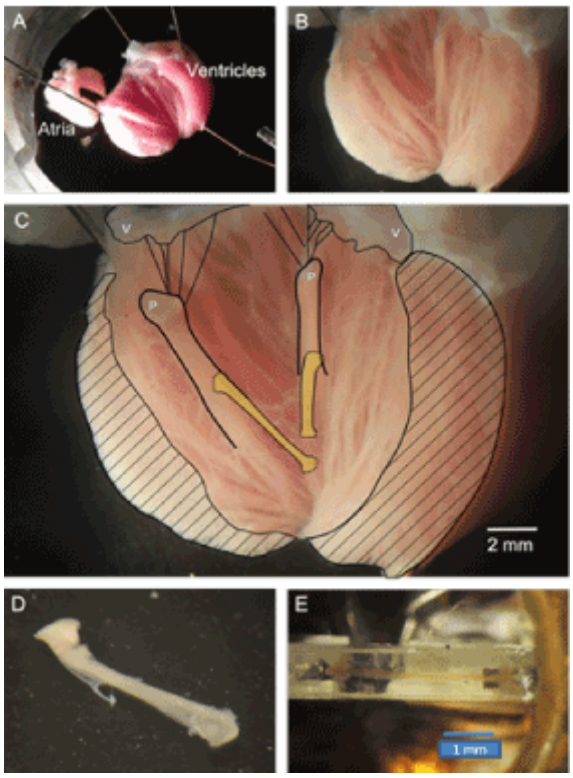

Figure 8: Photomontage of the steps involved in dissection of a rat LV trabecula and mounting it in the measurement chamber of our unique work-loop calorimeter. The LV chamber is exposed (A) and visually examined (B). Suitable trabeculae are identified (highlighted) – in this case arising from the free wall and inserting into the base of both papillary muscles (C). A preparation is dissected (D) and mounted, between hooks, in the glass measurement chamber of the microcalorimeter (see Figure 9 for details). [Reproduced from PhD Thesis of Soyeon (Eden) Goo [92].]

The rat isolated LV trabecula model

Trabeculae are minute, naturally arising, thread-like collections of linearly arranged myocytes (commonly 2-3 mm in length and 250 μm in diameter). This 'linear' microstructure largely eliminates any ambiguity in the measurement of extent of shortening and the development of force. For this reason, they have become the preparation-of-choice in the study of cardiac mechanics, since their introduction by ter Keurs et al. some 35 years ago [98]. In Figure 8, we present photographs of the steps involved in dissecting and mounting a suitable rat LV trabecula.

Work-loop microcalorimetry: Our laboratory has developed a unique device with which to drive trabeculae through force-length work-loops designed to measure the pressure-volume work-loops of the heart, while simultaneously measuring their heat output. This device [82], which we call a work-loop calorimeter, measures displacement in the order of micrometres, forces in the order of micrograms and heat output in the order of nanowatts. Displacement is achieved by a linear motor and is measured by one arm of a heterodyne laser. Another arm of the laser, using differential laser-Doppler techniques, measures the bending of a very stiff stainless-steel lever to provide a measure of force production (Figure 9). The product of force and displacement provides an estimate of external work performance.

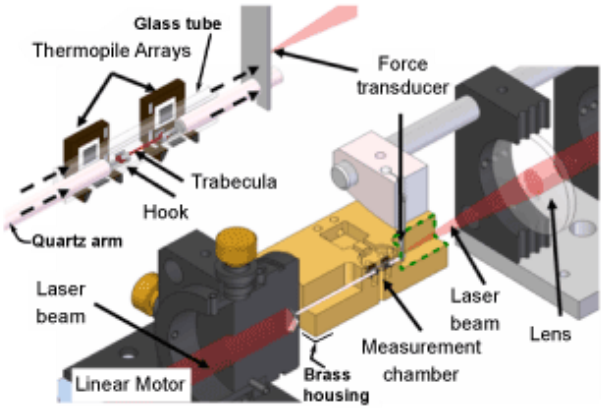

Figure 9: The work-loop micro-calorimeter. A trabecula is connected at either end, via platinum hooks, to glass rods and manoeuvred into a glass tube and located mid-way between arrays of external upstream and downstream arrays of thermopiles (see the Inset). The resulting 'measurement chamber' is located in a large brass block that acts as a thermal 'stabiliser'. The free end of the downstream glass rod is connected to the steel shaft that comprises the force transducer, while the other end is connected to a linear motor, the movement of which is effected via custom-written software. [Modified from Taberner et al. [82].]

The principal of heat measurement by the device is conceptually simple. The trabecula is tethered to 'upstream' and 'downstream' platinum hooks and located mid-stream. Since it is respiring and producing heat, the temperature of the downstream superfusate is higher than that upstream. This difference is sensed by arrays of thermopiles, the voltage outputs of which are proportional to the difference of temperature of the upstream and downstream superfusate (see the inset of Figure 9).

Knowing the rate of flow of the bathing solution and the temperature sensitivity of the thermopiles, it is straightforward to calculate the rate of heat production of the trabecula. With this facility, coupled with the ability to measure and control both force and shortening during a single muscle twitch, we can subject trabeculae to work-loops such as those exemplified in Figure 10. Note that these are force-length loops, designed to mimic the pressure-volume loops performed by the heart with each beat.

Work, heat and contractile efficiency of trabeculae: Typical experimental records from a 'work-loop experiment' are presented in Figure 10.

From records such as those presented in Figure 10, arising from an individual experiment, it is straightforward to calculate values of work, heat and efficiency, as functions of afterload.

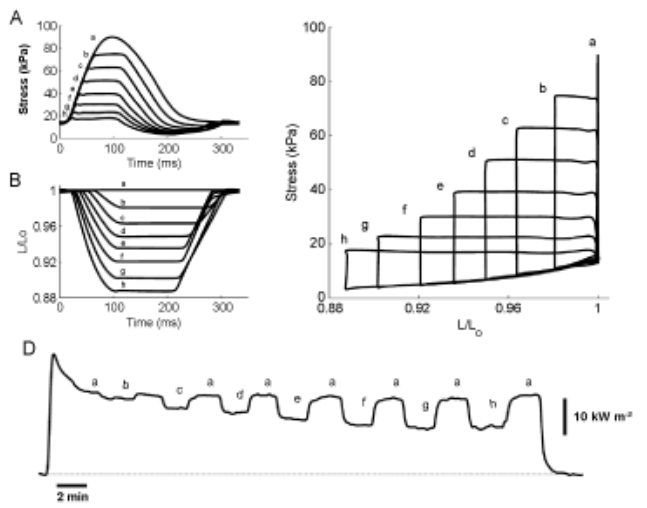

Figure 10: Twitch stress, length change and rate of heat production of isotonic work-loops. (A) Steady-state twitch stress of an isometric contraction (a) superimposed with workloop twitch stress profiles at various afterloads (b–h) of a representative trabecula. (B) Corresponding length changes throughout the timecourses of twitch stresses in A. (C) Parametric plots of the data in A against those in B. (D) Record of rate of heat production for 7 variouslyafterloaded workloop contractions (b–h), each bracketed by isometric contractions (a). [J-C Han: unpublished recordings.]

Repeating the procedure for a number of trabeculae allows us to calculate average values for each variable and, thus, to make statistical comparisons between diabetic and non-diabetic hearts. Examples of both individual (insets) and group results are displayed in Figure 11 where the thick lines denote STZ-treated hearts and the thin lines their controls.

It can be seen in Figure 11A that twitch heat production is linearly related to afterload. Hence, extrapolation of the line to the ordinate, where the magnitude of the force is zero, yields an estimate of the force-independent or 'activation' heat. As described, above, 'activation' is the name given to the processes that take place between the arrival of an action potential (i.e., depolarisation of the sarcolemmal membrane) and release of Ca^{2+} from its intracellular stores (the sarcoplasmic reticulum). Activation heat is the thermal accompaniment of the work of ion pumps that restore the cell to its diastolic ionic equilibrium. We estimate this value by quantifying the heat production in the absence of force production, i.e., the intercept of the heat-afterload relation.

It can also be seen in Figure 11A that the Work component is a modest fraction of the total Energy expenditure (note the double scale on the ordinate), implying equally modest values of efficiency. This implication is borne out by the data shown in Figure 11B, where it can be seen that the maximum value of total efficiency (which occurs at a relative afterload of about 0.4) is scarcely 17%. Since this index of 'total' efficiency includes the activation heat in the denominator of the ratio, the contractile efficiency of the crossbridges *per se* can be extracted by subtracting the activation heat from the total heat in the denominator of the efficiency ratio. When this is done, the result (Figure 11C) shows a peak value in the vicinity of 40%. As far as the crossbridges are concerned, the Activation Heat is pure 'overhead'.

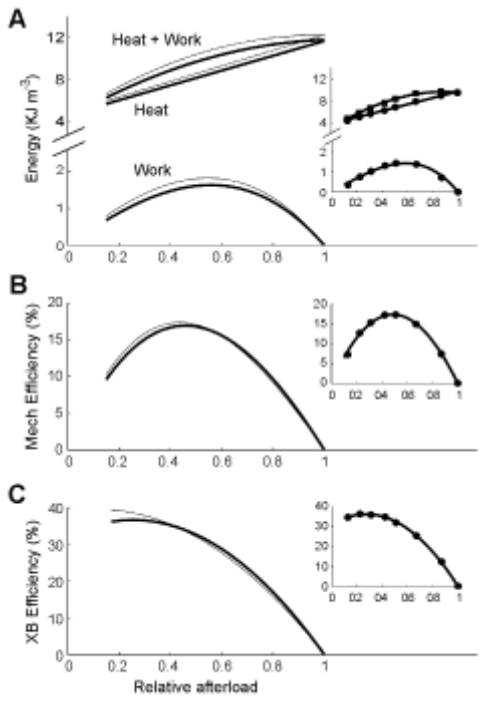

Figure 11: Average energy expenditure, work output and efficiency as functions of relative afterload of rat LV trabeculae. A: Work, heat and their sum (energy). Note use of two different scales on the ordinate. Extrapolation of the heat relation to the ordinate provides an estimate of Activation Heat. B: Mechanical ('Mech.') efficiency, the ratio of work to (work+heat) from A. C: subtraction of Activation Heat from the denominator of the expression for Total Efficiency reveals crossbridge (XB) efficiency. Thin lines denote average data from Control trabeculae; thick lines from trabeculae of STZ-treated rats. Insets: data from representative preparations. [Modified from Han et al. [99].]

An apparent paradox

Given the amount of information already gleaned from Figure 11, it is easy to overlook an apparent paradox. There is no difference of performance between trabeculae originating from diabetic hearts and controls. The dependencies on afterload of work output, heat evolution, total energy expenditure (work+heat), contractile efficiency and cross-bridge efficiency are indistinguishable between the two cohorts. At face value, these results contradict those observed in working whole-hearts. How can the peak twitch force of STZ trabeculae and their controls not differ in the 'one-dimensional' case of isolated trabeculae (Figure 11), when the peak afterload achievable by the 'three dimensional' whole-heart (Figure 7) is so severely compromised by diabetes? How is this contradiction to be reconciled?

The literature is replete with reports showing a constellation of consequences for the diabetic heart: prolongation of the duration of the action potential [100-104], thereby diminishing the period of electrical diastole, slowing the relaxation phase of the Ca^{2+} transient [79,80,105,106], thereby prolonging the 'activated state', and reducing activity of the actomyosin ATPase [107-112], consistent with a switch

from the α (fast twitch) to the β (slow twitch) isoform of the actomyosin ATPase [107,109,113-115]. Each of these phenomena contributes to prolongation of twitch duration and, effectively, an abbreviation of the period of mechanical diastole. Thus, at even physiological heart rates (4-5 Hz for the rat heart), the diastolic heart has less time to fill. Hence, its diastolic volume is reduced and, since the sarcomeres will now be operating at shorter length, peak systolic pressure development is reduced. By contrast, when an isolated trabecula undergoes a force-length loop, it is forcibly returned to L_o (optimal sarcomere length for developing force) during the diastolic interval. Realisation of this fundamental difference of diastolic behaviour allows reconciliation of the apparent contradiction. Diabetes does NOT reduce the ability of the tissues of the heart to develop force or pressure. The abbreviation of the diastolic period is the culprit. This insight could not have been gleaned had we not had experimental access to both whole-heart and isolated tissue preparations.

The Paradoxical Results between Mitochondrial (Input) Efficiency and Mechanical (Output) Efficiency

Despite resolving a contradiction between the behaviours of the intact heart and its tissues, we are nevertheless left with something of a contradiction. The efficiency of the mitochondria from diabetic hearts is about 15% lower than that of healthy hearts (Figure 2). But the peak efficiency of either intact diabetic hearts (Figure 7) or their trabeculae (Figure 11) is not. We can offer no definitive explanation but, given the resolution of the apparent contradiction outlined above, we are tempted to wonder if some equivalent phenomenon awaits for the measurement of mitochondrial efficiency. Is there some combination of concentrations of metabolic substrates that would allow submaximal rates of oxidative phosphorylation to yield equivalent P:O ratios between diabetic and non-diabetic hearts? As is invariably the case, more research is needed.

Summary and Conclusions

Provided with oxygen and metabolic substrates, the mitochondria, produce ATP. The efficiency of this oxidative phosphorylation (input) process can be quantified. The ATP produced can then be used to drive ion pumps in the sarcolemma and sarcoplasmic reticulum, and the relative sliding motion of the actin and myosin filaments. The efficiency of this overall 'activation-contraction' (output) process can also be measured–in either the isolated whole-heart or in samples of tissue dissected from it. We (and many others) observe that mitochondrial efficiency is depressed in the diabetic heart.

We find no difference in the peak output efficiency (i.e., the ratio of work to oxygen consumption) between STZ-diabetic and healthy hearts, although the mechanical output of the heart is reduced. This finding underscores the importance of examining cardiac mechano-energetics across a wide range of afterloads.

Measurement of the output efficiency (i.e., the ratio of work to (work plus heat)) of isolated trabeculae likewise reveals no difference between diabetic and healthy tissue. But, in striking contrast with the inability of the isolated whole heart to develop high left-ventricular pressures *in vitro*, there is no reduction in the ability of isolated trabeculae to produce maximal force. Resolution of this apparent conflict provides new insight into the mechanical behaviour of the diabetic heart *in vivo*. Dysfunction observed in the diabetic heart cannot be wholly attributed to a reduction of force development by myocardial tissues *per se* (at least at this time-point of diabetic insult) but, rather, involves complications at the whole organ level-most likely related to diminished chamber compliance. This result underscores the advantage of studying isolated organs and their tissues organs.

These investigations provide important clarification for the field of diabetic cardiac pathology by elucidating the effects of diabetes on cardiac efficiency and reconciling inconsistent findings in the literature. It is now clear that previous reports of a reduction in cardiac efficiency in diabetes can be explained by the fact that investigators have performed measurements at only a single afterload. By evaluating the effect of diabetes on cardiac efficiency over a range of afterloads, we now see that peak efficiency is not affected by diabetes, but the capacity of the diabetic heart to pump at high afterloads is diminished. Our experimental protocol (the use of crystalloid perfusates) may underestimate this effect with respect to blood-perfusion, since diabetes is known to increase the viscosity of serum [116]. These findings have important implications for understanding the mechanisms of cardiac dysfunction in diabetes and support the contention that targeting treatment interventions aimed at improving the efficiency of the diabetic heart may not be an effective approach but strategies for attenuating the shortened diastolic period should be pursued with vigour.

Acknowledgements

This study was supported by grants from the Health Research Council of New Zealand, the Royal Society of New Zealand, the National Heart Foundation of New Zealand, the Maurice and Phyllis Paykel Trust, and the FRDF funds of the Faculty of Engineering and Auckland Bioengineering Institute, and the Virtual Physiological Rat Centre funded through NIH (P50-GM094503).

References

1. Siegel K, Narayan KM (2008) The Unite for Diabetes campaign: overcoming constraints to find a global policy solution. Global Health 4: 3.
2. Lopaschuk GD (2002) Metabolic abnormalities in the diabetic heart. Heart Fail Rev 7: 149-159.
3. Miki T, Yuda S, Kouzu H, Miura T (2013) Diabetic cardiomyopathy: pathophysiology and clinical features. Heart Fail Rev 18: 149-166.
4. Feuvray D, Darmellah A (2008) Diabetes-related metabolic perturbations in cardiac myocyte. Diabetes Metab 34 Suppl 1: S3-9.
5. Schnell O, Cappuccio F, Genovese S, Standl E, Valensi P, et al. (2013) Type 1 diabetes and cardiovascular disease. Cardiovasc Diabetol 12: 156.
6. Gottlieb R (2012) Tragic heart, magic art. Heart Failure Reviews 18: 555.
7. Rubler S, Dlugash J, Yuceoglu YZ, Kumral T, Branwood AW, et al. (1972) New type of cardiomyopathy associated with diabetic glomerulosclerosis. Am J Cardiol 30: 595-602.
8. Boudina S, Abel ED (2010) Diabetic cardiomyopathy, causes and effects. Rev Endocr Metab Disord 11: 31-39.
9. Cooper GJ, Young AA, Gamble GD, Occleshaw CJ, Dissanayake AM, et al. (2009) A copper(II)-selective chelator ameliorates left-ventricular hypertrophy in type 2 diabetic patients: a randomised placebo-controlled study. Diabetologia 52: 715-722.
10. Fang ZY, Schull-Meade R, Downey M, Prins J, Marwick TH (2005) Determinants of subclinical diabetic heart disease. Diabetologia 48: 394-402.
11. Marwick TH (2008) Diabetic heart disease. Postgrad Med J 84: 188-192.
12. Patil VC, Patil HV, Shah KB, Vasani JD, Shetty P (2011) Diastolic dysfunction in asymptomatic type 2 diabetes mellitus with normal systolic function. J Cardiovasc Dis Res 2: 213-222.

13. Galderisi M (2006) Diastolic dysfunction and diabetic cardiomyopathy: evaluation by Doppler echocardiography. J Am Coll Cardiol 48: 1548-1551.
14. Liu JE, Palmieri V, Roman MJ, Bella JN, Fabsitz R, et al. (2001) The impact of diabetes on left ventricular filling pattern in normotensive and hypertensive adults: the strong heart study. J Am Coll Cardiol 37: 1943-1949.
15. van Heerebeek L, Hamdani N, Handoko ML, Falcao-Pires I, Musters RJ, et al. (2008) Diastolic stiffness of the failing diabetic heart: Importance of fibrosis, advanced glycation end products, and myocyte resting tension. Circulation 117: 43-51.
16. Zabalgoitia M, Ismaeil MF, Anderson L, Maklady FA (2001) Prevalence of diastolic dysfunction in normotensive, asymptomatic patients with well-controlled type 2 diabetes mellitus. Am J Cardiol 87: 320-323.
17. Boyer JK, Thanigaraj S, Schechtman KB, Pérez JE (2004) Prevalence of ventricular diastolic dysfunction in asymptomatic, normotensive patients with diabetes mellitus. Am J Cardiol 93: 870-875.
18. Brooks BA, Franjic B, Ban CR, Swaraj K, Yue DK, et al. (2008) Diastolic dysfunction and abnormalities of the microcirculation in type 2 diabetes. Diabetes Obes Metab 10: 739-746.
19. Albanna II, Eichelberger SM, Khoury PR, Witt SA, Standiford DA, et al. (1998) Diastolic dysfunction in young patients with insulin-dependent diabetes mellitus as determined by automated border detection. J Am Soc Echocardiogr 11: 349-355.
20. Nadeau KJ, Regensteiner JG, Bauer TA, Brown MS, Dorosz JL, et al. (2010) Insulin resistance in adolescents with Type 1 diabetes and its relationship to cardiovascular function. J Clin Endocrinol Metab 95: 513-521.
21. Salem M, El Behery S, Adly A, Khalil D, El Hadidi E (2009) Early predictors of myocardial disease in children and adolescents with type 1 diabetes mellitus. Pediatr Diabetes 10: 513-521.
22. Shah AM, Hung CL, Shin SH, Skali H, Verma A, et al. (2011) Cardiac structure and function, remodeling, and clinical outcomes among patients with diabetes after myocardial infarction complicated by left ventricular systolic dysfunction, heart failure, or both. Am Heart J 162: 685-691.
23. Pappachan JM, Varughese GI, Sriraman R, Arunagirinathan G (2013) Diabetic cardiomyopathy: Pathophysiology, diagnostic evaluation and management. World J Diabetes 4: 177-189.
24. Delbridge LM Loiselle DS (1981) An ultrastructural investigation into the size dependency of contractility of isolated cardiac muscle. Cardiovascular Research 15: 21-27.
25. Bessman SP, Carpenter CL (1985) The creatine-creatine phosphate energy shuttle. Annu Rev Biochem 54: 831-862.
26. McClellan G, Weisberg A, Winegrad S (1983) Energy transport from mitochondria to myofibril by a creatine phosphate shuttle in cardiac cells. Am J Physiol 245: C423-427.
27. MITCHELL P (1961) Coupling of phosphorylation to electron and hydrogen transfer by a chemi-osmotic type of mechanism. Nature 191: 144-148.
28. Petronilli V, Pietrobon D, Zoratti M, Azzone GF (1986) Free energy coupling between H+-generating and H+-consuming pumps. Ratio between output and input forces. Eur J Biochem 155: 423-431.
29. Futai M Kanazawa H (1983) Structure and function of proton-translocating adenosine triphosphatase (F0F1): biochemical and molecular biological approaches. Microbiol Rev 47: 285-312.
30. Boyer PD (1999) What makes ATP synthase spin? Nature 402: 247, 249.
31. Kato-Yamada Y, Noji H, Yasuda R, Kinosita K Jr, Yoshida M (1998) Direct observation of the rotation of epsilon subunit in F1-ATPase. J Biol Chem 273: 19375-19377.
32. Rich PR (2003) The molecular machinery of Keilin's respiratory chain. Biochem Soc Trans 31: 1095-1105.
33. Salway JS (2004) pages: Blackwell Publishing Ltd Oxford, UK.
34. Goo S, Pham T, Han JC, Nielsen P, Taberner A, et al. (2013) Multiscale measurement of cardiac energetics. Clin Exp Pharmacol Physiol 40: 671-681.
35. Iftikar FI, Hickey AJ (2013) Do mitochondria limit hot fish hearts? Understanding the role of mitochondrial function with heat stress in Notolabrus celidotus. PLoS One 8: e64120.
36. Hunter FW, Wang J, Patel R, Hsu H-L, Hickey AJR, Hay MP Wilson WR (2012) Homologous recombination repair-dependent cytotoxicity of the benzotriazine di-N-oxide CEN-209: Comparison with other hypoxia-activated prodrugs. Biochemical Pharmacology 83: 574-585.
37. Kuznetsov AV, Veksler V, Gellerich FN, Saks V, Margreiter R, et al. (2008) Analysis of mitochondrial function in situ in permeabilized muscle fibers, tissues and cells. Nat Protoc 3: 965-976.
38. Gnaiger E (2008) Polarographic oxygen sensors, the oxygraph and high-resolution respirometry to assess mitochondrial function. John Wiley & Sons, Inc, Hoboken NJ, pp-327-352.
39. Gnaiger E (2009) Capacity of oxidative phosphorylation in human skeletal muscle: new perspectives of mitochondrial physiology. Int J Biochem Cell Biol 41: 1837-1845.
40. Lemieux H, Votion M-D Gnaiger E (2011) Mitochondrial respiration in premeabilized fibres: needle biopsies from horse skeletal muscle. Mitochondrial Physiology Network 12: 1-4.
41. Pesta D Gnaiger E (2012) High-Resolution Respirometry: OXPHOS Protocols for Human Cells and Permeabilized Fibers from Small Biopsies of Human Muscle. Methods Mol Biol 810: 25-5
42. Gnaiger E (2007) Mitochondrial pathways and respiratory control. OROBOS MiPNet, Innisbruck, Austria 1-98.
43. Buchanan J, Mazumder PK, Hu P, Chakrabarti G, Roberts MW (2005) Reduced Cardiac Efficiency and Altered Substrate Metabolism Precedes the Onset of Hyperglycemia and Contractile Dysfunction in Two Mouse Models of Insulin Resistance and Obesity. Endocrinology 146: 5341-5349.
44. Mazumder PK, O'Neill BT, Roberts MW, Buchanan J, Yun UJ, et al. (2004) Impaired cardiac efficiency and increased fatty acid oxidation in insulin-resistant ob/ob mouse hearts. Diabetes 53: 2366-2374.
45. Wang P, Lloyd SG, Zeng H, Bonen A, Chatham JC (2005) Impact of altered substrate utilization on cardiac function in isolated hearts from Zucker diabetic fatty rats. Am J Physiol Heart Circ Physiol 288: H2102-2110.
46. Brand MD, Affourtit C, Esteves TC, Green K, Lambert AJ, et al. (2004) Mitochondrial superoxide: production, biological effects, and activation of uncoupling proteins. Free Radic Biol Med 37: 755-767.
47. Brand MD Esteves TC (2005) Physiological functions of the mitochondrial uncoupling proteins UCP2 and UCP3. Cell Metab 2: 85-93.
48. Boudina S, Sena S, O'Neill BT, Tathireddy P, et al. (2005) Reduced mitochondrial oxidative capacity and increased mitochondrial uncoupling impair myocardial energetics in obesity. Circulation 112: 2686-2695.
49. Hickey AJR, Chai CC, Choong SY, de Freitas Costa S, Skea GL, et al. (2009) Impaired ATP turnover and ADP supply depress cardiac mitochondrial respiration and elevate superoxide in nonfailing spontaneously hypertensive rat hearts. Am J Physiol Cell Physiol 297: C766-C774.
50. Bugger H Abel ED (2008) Molecular basis of cardiac efficiency. Heart Metabolism 39: 5-9.
51. Brown GC, Borutaite V (2007) Nitric oxide and mitochondrial respiration in the heart. Cardiovasc Res 75: 283-290.
52. Peralta GJ Poderoso JJ (2006) Role of nitric oxide and mitochondrial nitric oxide synthase in energy adaptive responses. Current Cardiology Reviews 2: 193-204.
53. Bugger H, Abel ED (2010) Mitochondria in the diabetic heart. Cardiovasc Res 88: 229-240.
54. Anderson EJ, Kypson AP, Rodriguez E, Anderson CA, Lehr EJ, et al. (2009) Substrate-specific derangements in mitochondrial metabolism

and redox balance in the atrium of the type 2 diabetic human heart. J Am Coll Cardiol 54: 1891-1898.

55. Boudina S, Sena S, Theobald H, Sheng X, Wright JJ, Hu XX, Aziz S, Johnson JI, Bugger H, et al. (2007) Mitochondrial energetics in the heart in obesity-related diabetes: Direct evidence for increased uncoupled respiration and activation of uncoupling proteins. Diabetes 56: 2457-2466.
56. Jüllig M, Hickey AJ, Middleditch MJ, Crossman DJ, Lee SC, et al. (2007) Characterization of proteomic changes in cardiac mitochondria in streptozotocin-diabetic rats using iTRAQâ„¢ isobaric tags. Proteomics Clin Appl 1: 565-576.
57. Bugger H, Boudina S, Hu XX, Tuinei J, Zaha VG, et al. (2008) Type 1 diabetic akita mouse hearts are insulin sensitive but manifest structurally abnormal mitochondria that remain coupled despite increased uncoupling protein 3. Diabetes 57: 2924-2932.
58. Chinopoulos C, Vajda S, Csanády L, Mándi M, Mathe K, et al. (2009) A novel kinetic assay of mitochondrial ATP-ADP exchange rate mediated by the ANT. Biophys J 96: 2490-2504.
59. Kovács M, Tóth J, Hetényi C, Málnási-Csizmadia A, Sellers JR (2004) Mechanism of blebbistatin inhibition of myosin II. J Biol Chem 279: 35557-35563.
60. Murphy MP (2009) How mitochondria produce reactive oxygen species. Biochem J 417: 1-13.
61. Hickey AJR, Renshaw GMC, Speers-Roesch B, Richards JG, Wang Y et al. (2012) A radical approach to beating hypoxia: Depressed free radical release from heart fibres of the hypoxia-tolerant epaulette shark (Hemiscyllum ocellatum). J Comp Physiol 182: 91-100.
62. PARKS RE Jr, ADLER J, COPENHAVER JH Jr (1955) The efficiency of oxidative phosphorylation in mitochondria from diabetic rats. J Biol Chem 214: 693-698.
63. Pierce GN, Dhalla NS (1985) Heart mitochondrial function in chronic experimental diabetes in rats. Can J Cardiol 1: 48-54.
64. Kuo TH, Moore KH, Giacomelli F Wiener J (1983) Defective Oxidative Metabolism of Heart Mitochondria from Genetically Diabetic Mice. Diabetes 32: 781-787.
65. Flarsheim CE, Grupp IL Matlib MA (1996) Mitochondrial dysfunction accompanies diastolic dysfunction in diabetic rat heart. American Journal of Physiology - Heart and Circulatory Physiology 271: H192-H202.
66. Smith BK, Perry CG, Herbst EA, Ritchie IR, Beaudoin MS, et al. (2013) Submaximal ADP-stimulated respiration is impaired in ZDF rats and recovered by resveratrol. J Physiol 591: 6089-6101.
67. Beaudoin MS, Perry CCR, Arkell A, Chabowski A, Simpson JA (2014) In the ZDF rat, impairments in mitochondrial palmitoyl-CoA respiratory kinetics that precede the development of diabetic cardiomyopathy are prevented by resveratrol supplementation. The Journal of Physiology.
68. Randle PJ, Newsholme EA Garland PB (1964) Regulation of glucose uptake by muscle. 8. Effects of fatty acids, ketone bodies and pyruvate, and of alloxan-diabetes and starvation, on the uptake and metabolic fate of glucose in rat heart and diaphragm muscles. Biochemical Journal 93: 652-665.
69. Herrero P, Peterson LR, McGill JB, Matthew S, Lesniak D, et al. (2006) Increased myocardial fatty acid metabolism in patients with type 1 diabetes mellitus. J Am Coll Cardiol 47: 598-604.
70. Boudina S, Abel ED (2006) Mitochondrial uncoupling: a key contributor to reduced cardiac efficiency in diabetes. Physiology (Bethesda) 21: 250-258.
71. Boudina S, Abel ED (2007) Diabetic cardiomyopathy revisited. Circulation 115: 3213-3223.
72. Murphy MP (2009) How mitochondria produce reactive oxygen species. Biochem J 417: 1-13.
73. Mellor K, Ritchie RH, Meredith G, Woodman OL, Morris MJ, et al. (2010) High-fructose diet elevates myocardial superoxide generation in mice in the absence of cardiac hypertrophy. Nutrition 26: 842-848.
74. Mellor KM, Ritchie RH, Davidoff AJ, Delbridge LM (2010) Elevated dietary sugar and the heart: experimental models and myocardial remodeling. Can J Physiol Pharmacol 88: 525-540.
75. Steinberger J Daniels SR (2003) Obesity, insulin resistance, diabetes, and cardiovascular risk in children. An American Heart Association scientific statement from the Atherosclerosis, Hypertension, and Obesity in the Young Committee (Council on Cardiovascular Disease in the Young) and the Diabetes Committee (Council on Nutrition, Physical Activity, and Metabolism). Circulation 107: 1448-1453.
76. Lopaschuk GD, Katz S McNeill JH (1983) The effect of alloxan- and streptozotocin-induced diabetes on calcium transport in rat cardiac sarcoplasmic reticulum. The possible involvement of long chain acylcarnitines. Can J Physiol Pharmacol 61: 398-448.
77. Xiang H, McNeill JH (1990) Calcium uptake activity of cardiac sarcoplasmic reticulum in myo-inositol-treated diabetic rats. Gen Pharmacol 21: 251-254.
78. Cesario DA, Brar R, Shivkumar K (2006) Alterations in ion channel physiology in diabetic cardiomyopathy. Endocrinol Metab Clin North Am 35: 601-610, ix-x.
79. Zhang L, Ward M-L, Phillips ARJ, Zhang S, Kennedy J et al. (2013) Protection of the heart by treatment with a divalent-copper-selective chelator reveals a novel mechanism underlying cardiomyopathy in diabetic rats. Cardiovascular Diabetology 12: 1-17.
80. Zhang L, Cannell MB, Phillips AR, Cooper GJ, Ward ML (2008) Altered calcium homeostasis does not explain the contractile deficit of diabetic cardiomyopathy. Diabetes 57: 2158-2166.
81. Goo S, Han J-C, Nisbet LA, LeGrice IJ, Taberner AJ et al. (2014) Dietary pre-exposure of rats to fish oil does not enhance myocardial efficiency of isolated working-hearts or their left ventricular trabeculae. Journal of Physiology (London) 592: 1795-1808.
82. Taberner AJ, Han JC, Loiselle DS, Nielsen PM (2011) An innovative work-loop calorimeter for in vitro measurement of the mechanics and energetics of working cardiac trabeculae. J Appl Physiol (1985) 111: 1798-1803.
83. Han JC, Taberner AJ, Nielsen PM, Loiselle DS (2013) Interventricular comparison of the energetics of contraction of trabeculae carneae isolated from the rat heart. J Physiol 591: 701-717.
84. Han J-C, Goo S, Barrett CJ, Mellor KM, Taberner AJ Loiselle DS (2014) The afterload-dependent peak efficiency of the isolated working rat heart is unaffected by streptozotocin-induced diabetes. Cardiavascular Diabetology 13: 4.
85. Khalafbeigui F, Suga H, Sagawa K (1979) Left ventricular systolic pressure-volume area correlates with oxygen consumption. Am J Physiol 237: H566-569.
86. Suga H (1979) Total mechanical energy of a ventricle model and cardiac oxygen consumption. Am J Physiol 236: H498-505.
87. Suga H, Hayashi T, Shirahata M, Ninomiya I (1980) Critical evaluation of left ventricular systolic pressure volume areas as predictor of oxygen consumption rate. Jpn J Physiol 30: 907-919.
88. Suga H, Hayashi T, Shirahata M (1981) Ventricular systolic pressure-volume area as predictor of cardiac oxygen consumption. Am J Physiol 240: H39-44.
89. Suga H (1990) Ventricular energetics. Physiol Rev 70: 247-277.
90. Han JC1, Taberner AJ, Tran K, Goo S, Nickerson DP, et al. (2012) Comparison of the Gibbs and Suga formulations of cardiac energetics: the demise of "isoefficiency". J Appl Physiol (1985) 113: 996-1003.
91. Han JC, Taberner AJ, Tran K, Nickerson DP, Nash MP, et al. (2012) Relating components of pressure-volume area in Suga's formulation of cardiac energetics to components of the stress-time integral. J Appl Physiol (1985) 113: 988-995.
92. Goo S (2014) Does Dietary Fish Oil Enhance Myocardial Efficiency? PhD Thesis. Department of Physiology and Auckland Bioengineering Institute, The University of Auckland.
93. Guild SJ, Ward ML, Cooper PJ, Hanley PJ, Loiselle DS (2003) Extracellular Ca2+ is obligatory for ouabain-induced potentiation of

cardiac basal energy expenditure. Clin Exp Pharmacol Physiol 30: 103-109.

94. Ward ML, Cooper PJ, Hanley PJ, Loiselle DS (2003) Species-independent metabolic response to an increase of [Ca(2+)](i) in quiescent cardiac muscle. Clin Exp Pharmacol Physiol 30: 586-589.
95. Burkhoff D, Kalil-Filho R, Gerstenblith G (1990) Oxygen consumption is less in rat hearts arrested by low calcium than by high potassium at fixed flow. Am J Physiol 259: H1142-1147.
96. Mikane T, Araki J, Suzuki S, Mizuno J, Shimizu J, et al. (1999) O(2) cost of contractility but not of mechanical energy increases with temperature in canine left ventricle. Am J Physiol 277: H65-73.
97. Saeki A, Goto Y, Hata K, Takasago T, Nishioka T, et al. (2000) Negative inotropism of hyperthermia increases oxygen cost of contractility in canine hearts. Am J Physiol Heart Circ Physiol 279: H2855-2864.
98. ter Keurs HE, Rijnsburger WH, van Heuningen R, Nagelsmit MJ (1980) Tension development and sarcomere length in rat cardiac trabeculae. Evidence of length-dependent activation. Circ Res 46: 703-714.
99. Han J-C, Tran K, Nielsen PMF, Taberner AJ Loiselle DS (2014) Streptozotocin-induced diabetes prolongs twitch duration without affecting the energetics of isolated ventricular trabeculae. Cardiovascular Diabetology 13: 1-16.
100. Nobe S, Aomine M, Arita M, Ito S Takaki R (1990) Chronic diabetes mellitus prolongs action potential duration of rat ventricular muscles: circumstantial evidence for impaired Ca2+ channel. Cardiovascular Research 24: 381-389.
101. Fein FS, Aronson RS, Nordin C, Miller-Green B, Sonnenblick EH (1983) Altered myocardial response to ouabain in diabetic rats: mechanics and electrophysiology. J Mol Cell Cardiol 15: 769-784.
102. Yuill KH, Tosh D, Hancox JC (2010) Streptozotocin-induced diabetes modulates action potentials and ion channel currents from the rat atrioventricular node. Exp Physiol 95: 508-517.
103. Jourdon P, Feuvray D (1993) Calcium and potassium currents in ventricular myocytes isolated from diabetic rats. J Physiol 470: 411-429.
104. Magyar J, Rusznák Z, Szentesi P, Szûcs G, Kovács L (1992) Action potentials and potassium currents in rat ventricular muscle during experimental diabetes. J Mol Cell Cardiol 24: 841-853.
105. Kotsanas G, Delbridge LM, Wendt IR (2000) Stimulus interval-dependent differences in Ca2+ transients and contractile responses of diabetic rat cardiomyocytes. Cardiovasc Res 46: 450-462.
106. Yaras N, Ugur M, Ozdemir S, Gurdal H, Purali N, et al. (2005) Effects of diabetes on ryanodine receptor Ca release channel (RyR2) and Ca2+ homeostasis in rat heart. Diabetes 54: 3082-3088.
107. Dillmann WH (1980) Diabetes mellitus induces changes in cardiac myosin of the rat. Diabetes 29: 579-582.
108. Fein FS, Strobeck JE, Malhotra A, Scheuer J, Sonnenblick EH (1981) Reversibility of diabetic cardiomyopathy with insulin in rats. Circ Res 49: 1251-1261.
109. Malhotra A, Penpargkul S, Fein FS, Sonnenblick EH, Scheuer J (1981) The effect of streptozotocin-induced diabetes in rats on cardiac contractile proteins. Circ Res 49: 1243-1250.
110. Pierce GN, Dhalla NS (1981) Cardiac myofibrillar ATPase activity in diabetic rats. J Mol Cell Cardiol 13: 1063-1069.
111. Garber DW, Neely JR (1983) Decreased myocardial function and myosin ATPase in hearts from diabetic rats. Am J Physiol 244: H586-591.
112. Malhotra A, Lopez MC, Nakouzi A (1995) Troponin subunits contribute to altered myosin ATPase activity in diabetic cardiomyopathy. Mol Cell Biochem 151: 165-172.
113. Takeda N, Nakamura I, Hatanaka T, Ohkubo T, Nagano M (1988) Myocardial mechanical and myosin isoenzyme alterations in streptozotocin-diabetic rats. Jpn Heart J 29: 455-463.
114. Rupp H, Elimban V, Dhalla NS (1994) Modification of myosin isozymes and SR Ca(2+)-pump ATPase of the diabetic rat heart by lipid-lowering interventions. Mol Cell Biochem 132: 69-80.
115. Aragno M, Mastrocola R, Ghé C, Arnoletti E, Bassino E, et al. (2012) Obestatin induced recovery of myocardial dysfunction in type 1 diabetic rats: underlying mechanisms. Cardiovasc Diabetol 11: 129.
116. McMillan DE (1974) Disturbance of serum viscosity in diabetes mellitus. J Clin Invest 53: 1071-1079.